International Journal of Abrasive Technology

ISSN online: 1752-265X - ISSN print: 1752-2641
https://www.inderscience.com/ijat

Tangential dressing of diamond grinding wheel by femto-second pulsed laser with Bessel beam

Jiabin Zhou, Dongkai Chu, Peng Yao, Xiyong Jin, Lianjun Zhao, Yueming Li, Shitong Liang, Jimiao Xu, Shuoshuo Qu, Chuanzhen Huang

DOI: 10.1504/IJAT.2023.10054192

Article History:

Received:	08 July 2022
Last revised:	20 November 2022
Accepted:	14 December 2022
Published online:	12 May 2023

Tangential dressing of diamond grinding wheel by femto-second pulsed laser with Bessel beam

Jiabin Zhou and Dongkai Chu

Center for Advanced Jet Engineering Technologies (CaJET),
School of Mechanical Engineering,
Shandong University,
Jinan, 250061, China
Email: 1140519299@qq.com
Email: chudongkai@sdu.edu.cn

Peng Yao*

Center for Advanced Jet Engineering Technologies (CaJET),
School of Mechanical Engineering,
Shandong University,
Jinan, 250061, China
and
Shenzhen Research Institute,
Shandong University,
Shenzhen, 518063, China
Fax: +86-532-88392118
Email: yaopeng@sdu.edu.cn
*Corresponding author

Xiyong Jin and Lianjun Zhao

Goertek Inc.,
Weifang, 261041,
Shandong, China
Email: Justop.jin@goertek.com
Email: Bruce.zhao@goertek.com

Yueming Li, Shitong Liang and Jimiao Xu

Beijing Institute of Control Engineering,
Beijing, 100190, China
Email: 13681010911@139.com
Email: liangshitong@yahoo.cn
Email: xujimiao@163.com

Shuoshuo Qu

Center for Advanced Jet Engineering Technologies (CaJET),
School of Mechanical Engineering,
Shandong University,
Jinan, 250061, China
Email: qushuoshuo@sdu.edu.cn

Chuanzhen Huang

School of Mechanical Engineering,
Yanshan University,
Qinhuangdao, 066004,
Hebei, China
Email: huangchuanzhen@ysu.edu.cn

Abstract: Bronze bonded diamond grinding wheel is widely used in grinding hard and brittle materials. In order to improve the profile accuracy of the grinding wheel, an ultra-fast laser dressing method with Bessel beam for diamond grinding wheel is proposed in this study. The coarse grain (100 #) bronze bonded diamond grinding wheel is tangentially shaped by laser dressing. By comparing the profile and surface quality of the grinding wheel dressed with Gaussian laser beam and Bessel laser beam under different defocusing amounts, it is found that Bessel beam can dress the grinding wheel in the focal depth of 1.2 mm, which is three times of traditional Gaussian beam. The ablation thresholds of bronze binder and diamond under Bessel beam are obtained through experiments and theoretical calculations. The results show that when the laser power density is 3.75×10^5 W/cm^2 – 4.75×10^5 W/cm^2 and the axial scanning speed of the laser is 0.03 mm/min, the diamond grit has an enough protrusion height, and the runout of the grinding wheel is reduced to about 6 μm. When the wheel speed is too low, it will reduce the overlap rate of axial scanning trajectory and reduce the removal efficiency of material.

Keywords: bronze bond diamond grinding wheel; laser dressing; Bessel beam; defocusing amount; material removal; abrasive protrusion height; removal efficiency.

Reference to this paper should be made as follows: Zhou, J., Chu, D., Yao, P., Jin, X., Zhao, L., Li, Y., Liang, S., Xu, J., Qu, S. and Huang, C. (2023) 'Tangential dressing of diamond grinding wheel by femto-second pulsed laser with Bessel beam', *Int. J. Abrasive Technology*, Vol. 11, No. 3, pp.212–232.

Biographical notes: Jiabin Zhou received his MS in Mechanical Engineering at Shandong University. His researches focus on ultra-precision grinding and ultra-fast laser dressing of grinding wheel.

Dongkai Chu is an Assistant Professor in Mechanical Engineering at Shandong University. His researches focus on ultra-fast laser micro-nano fabrication and preparation of bionic absorbing functional surface.

Peng Yao is an Associate Dean and Professor in Mechanical Engineering at Shandong University. His research interest is the theory and technology of multi-energy assisted ultra-precision and high-efficiency machining of difficult-to-machine optical materials.

Xiyong Jin works as the Head of the Optical Research and Development Center at Goertek Inc., and his researches focus on optical ultra-precision machining technology and automation equipment.

Lianjun Zhao works as the Chief Designer of Intelligent Wearable Equipment at Goertek Inc. His researches focus on non-standard automation equipment, flexible production line and intelligent manufacturing.

Yueming Li is a Senior Engineer and works at Beijing Institute of Control Engineering. His researches focus on precision and ultra-precision machining technology, special machining technology.

Shitong Liang works at Beijing Institute of Control Engineering. His researches focus on the design of spacecraft optical sensor.

Jimiao Xu works at Beijing Institute of Control Engineering. His researches focus on Precision and ultra-precision manufacturing of spacecraft control system actuators and optical sensors.

Shuoshuo Qu is an Assistant Professor in Mechanical Engineering at Shandong University. His researches focus on precision and ultra-precision machining; green processing and composite material removal mechanism.

Chuanzhen Huang is a Professor in Mechanical Engineering at Yanshan University. His researches focus on high efficiency and precision machining technologies, precision abrasive air/waterjet micro-machining technologies, advanced ceramic tool materials and structural ceramics, and machining technologies for novel materials.

This paper is a revised and expanded version of a paper entitled ‘Tangential dressing of diamond grinding wheel by femto-second pulsed laser with Bessel beam’ presented at The 24th International Symposium on Advances in Abrasive Technology, Guangzhou, 9–12 December 2022.

1 Introduction

Bronze bonded diamond grinding wheel is sintered with diamond as abrasive and bronze as bond. Because of its excellent grinding performance and strong wear resistance, it is widely used in the grinding process of difficult-to-machine materials such as glass fibre reinforced plastics, engineering ceramics and cemented carbide (Weingaertner et al., 2010; Guo et al., 2016; Zhao and Guo, 2011; Xie and Dang, 2008). During the installation and use of the grinding wheel, the circular run-out error of it may be too large, and the grains may become blunt, which requires further dressing to ensure the profiling accuracy and the sharpness of the grinding wheel. However, due to the high hardness of diamond grinding wheels, there are great difficulties in its processing and dressing (Wegener et al., 2011; Chen et al., 2016; Guo et al., 2014b). Grinding wheel dressing includes two steps including profiling and sharpening (Deng et al., 2014b; Dražumeric et al., 2018; Zhou et al., 2019; Zhang et al., 2019). Profiling refers to the removal of materials (including diamond and binder) on the surface of the grinding wheel to obtain the required geometric accuracy of the grinding wheel. Sharpening refers to the removal of the binder on the surface of the grinding wheel to ensure the protrusion of the

abrasive grains (the best effect is obtained when the protrusion height of the abrasive grains is about 30%), resulting in enough debris space between the abrasive grains to achieve the function of grinding wheel (Chen et al., 2015b; Yao et al., 2018; Guo et al., 2018). When the traditional mechanical dressing technology is used to dress the bronze bonded diamond grinding wheel, due to the large mechanical force between the dressing tool and the grinding wheel, some problems such as large loss of the dressing tool, low accuracy, high cost and serious environmental pollution will be induced. When electrochemical modification is adopted, it is difficult to remove diamond particles due to the non-conductivity of diamond particles, resulting in low dressing efficiency and narrow application range (Deng et al., 2014a; Chen et al., 2005, 2013; Guo et al., 2014a).

As a new type of non-contact machining method, laser dressing avoids mechanical force and the wear of dressing tools in the dressing process (Yung et al., 2003; Jackson et al., 2003; Cai et al., 2017; Okamoto et al., 2019). Because abrasive particles and binders can be selectively removed by laser processing. Laser dressing can be applied to the dressing of any types of super-hard abrasive grinding wheels such as complex curved surface forming grinding wheels, ultra-thin grinding wheel cutting, and parallel grinding wheels. It is an advanced machining technology for precision dressing of diamond grinding wheels (Chen et al., 2015a; Du et al., 2016). The laser dressing technology uses the focused laser beam to scan the whole surface of the grinding wheel, and selectively removes the material on the surface of the grinding wheel to achieve the required size and profile accuracy of the grinding wheel (Deng et al., 2016; Zhang et al., 2016; Deng and Zhou, 2019). At present, scholars carried out many researches on the laser tangential shaping and radial dressing of the grinding wheel. For example, Dold et al. (2011) carried out the research on the tangential dressing of electroplated nickel-based single-layer diamond grinding wheel by using a pulse laser with wavelength of 1,030 nm and pulse duration of 10 ps, which proved the feasibility of the tangential dressing of electroplated nickel-based single-layer diamond grinding wheel by picosecond pulse laser. Walter et al. (2012) used a pulsed laser with a wavelength of 1,064 nm, a pulse frequency of 50 kHz and a pulse duration of less than 200 ns to carry out the laser tangential dressing experiment of the metal-ceramic composite binder CBN forming grinding wheel, shaping the complex profile of the corner arc radius of the surface groove less than 20 μm; Chen et al. (2019) and Deng et al. (2019) used nanosecond pulsed fibre laser to conduct tangential dressing experiment on the profile of 150 # bronze bond diamond grinding wheel, and optimised the key process parameters to improve the quality, accuracy and efficiency of pulsed laser dressing. Guo et al. (2022) and Liu et al. (2017) used pulsed laser to study the tangential shaping of V-shaped CBN grinding wheel, and established a theoretical model of pulsed laser profiling. By analysing the influence of grinding wheel speed and dressing time on the dressing effect, the angle of V-shaped grinding wheel can reach 90.15°, and the bottom fillet radius is 53 μm. Compared with mechanical dressing, the dressing time is greatly reduced. In addition, Hosokawa et al. (2006) from Kanazawa University carried out the experiment of radial dressing of bronze bond diamond grinding wheel with Nd: YAG pulsed laser, and the normal and tangential grinding forces during grinding with pulsed laser dressed diamond grinding wheel and white corundum grinding wheel were almost equal. Xie et al. (2004) used Nd: YAG laser with pulse duration of 150–500 nm to orthogonally modify the resin-based diamond wheel with particle size of 180 #, and obtained that the combination of laser parameters with low average power, medium pulse repetition rate and focusing position could obtain better surface

morphology. Because the laser is continuous in the incident direction and has no cutting edge like the cutting tools and grinding wheels, it is quite complex to control the depth of material removal with removal function in laser radial machining. During laser dressing, the profile of the grinding wheel changes in real time, while the focal depth of the ordinary Gaussian beam is too small. In the dressing process, the relative position between the focal point and the grinding wheel needs to be adjusted at all times, and the dressing efficiency is low (Liu et al., 2020; Bathe et al., 2014; Ackerl et al., 2020). Compared with Gaussian laser beam, Bessel laser beam can maintain a constant profile in a longer propagation direction (Meyer et al., 2020; Chu et al., 2019, 2020), which can reduce the requirement for the relative position between the focal spot and the workpiece in the machining process. However, there is no report on the grinding wheel dressing using Bessel beam.

To solve the above problems, this study proposes an ultra-short pulsed femto-second laser dressing method with Bessel beam. Because the femto-second pulsed lasers possess short heat affected zones, it is used to process a broad variety of materials such as metals, semiconductors, biological samples, etc. with very high degree of precision and reproducibility (Alexeev et al., 2010), and the materials have a high absorptivity at this wavelength, so we select this laser. The effects of laser power, axial scanning speed, wheel speed and scanning times on laser dressing are studied. The removal effect of abrasive particles and binder on diamond grinding wheel is evaluated, and the precision dressing experiments of grinding wheel are carried out by pulse laser with optimised parameters. This study provides a new method for increasing the efficiency an accuracy of laser dressing of grinding wheel.

2 Experimental apparatus and method

2.1 Experimental apparatus

The diamond grinding wheel (diameter D = 10 mm, width W = 20 mm, particle size 100 #, supplied by Kunshan Shuozhan Electronic Technology Co., Ltd) is tangential dressed by femto-second laser (Spectra Physics Spitfire Ace Ti sapphire laser system, pulse duration W = 35 fs, wavelength λ = 800 nm, repetition frequency PRF = 1 kHz, peak power 12 W). The physical properties of bronze bonded diamond grinding wheel are shown in Table 1 (Chen et al., 2010; Mei et al., 2009).

Table 1 Physical properties of bronze bond diamond grinding wheels

Property	*Diamond*	*Bronze bond*
Thermal conductivity λ/(W/(m·k))	2,000	41.9
Specific heat c/(J/(kg·K))	1,827	352
Thermal diffusivity α/($\times 10^{-4}$ m^2·s^{-1})	3.114	0.14
Vaporisation temperature T_v/K	3,550	2,770
Absorptivity A	0.15	0.38
Density ρ/(kg·m^3)	3,515	8,620

Figure 1 (a) Schematic diagram of optical path shaping of Bessel beam (b) Geometrical light path diagram of an axicon for generate a Bessel beam (c) Schematic diagram of a telescope system for improving Bessel optical power density (d) Schematic diagram of tangential dressing of grinding wheel (see online version for colours)

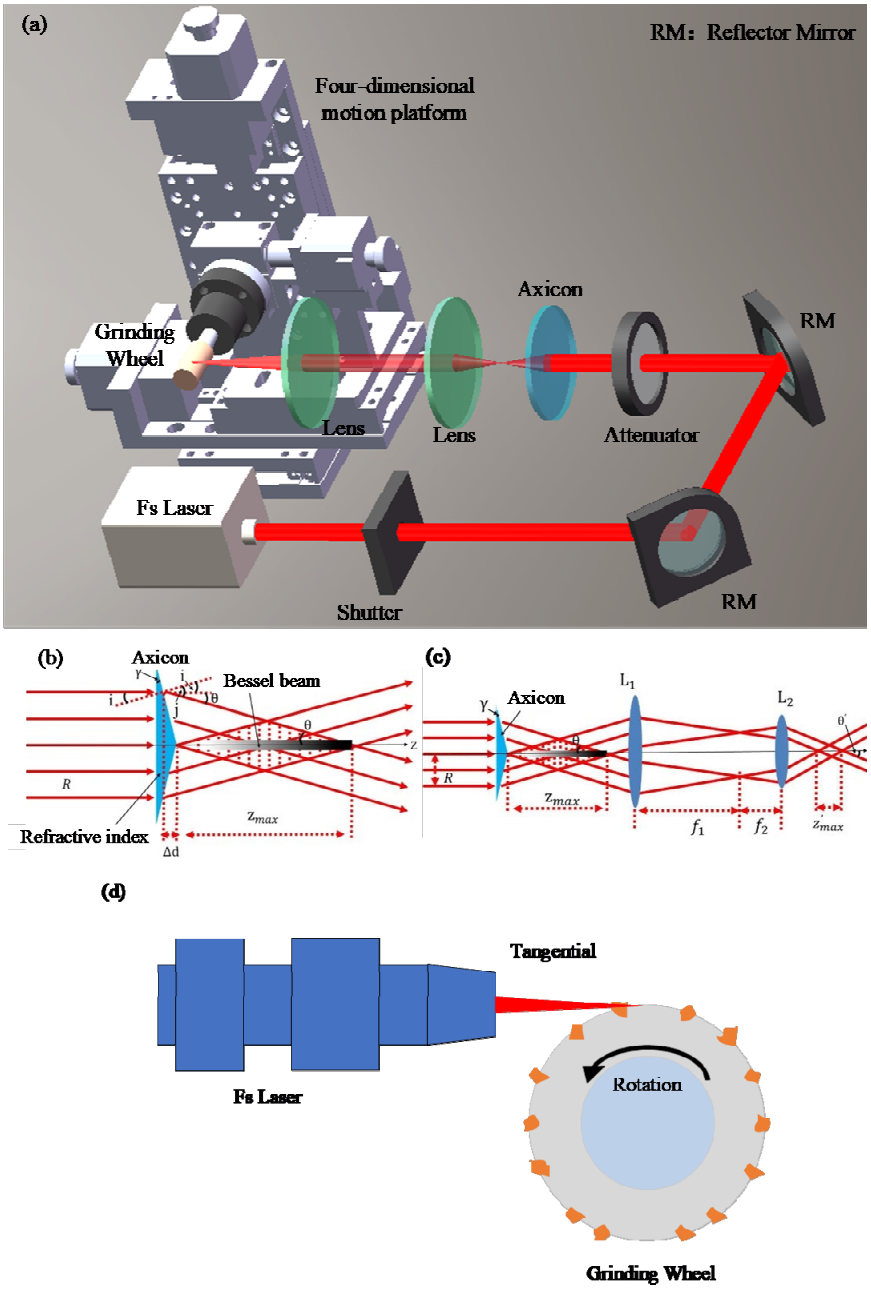

Figure 1(a) is the schematic diagram of tangential dressing of ultra-fast laser grinding wheel using Bessel laser beam. The laser used in processing has a central wavelength of

800 nm, a pulse duration of 35 fs, a repetition rate of 1 kHz, and a horizontal polarisation. In order to realise a long focal depth of laser beam, Gaussian beam was shaped into Bessel beam (all optical elements used in this experiment are provided by Daheng Optics). The laser first passes through the optical gate (controlling the on-off of the optical path system to determine the number of pulses in the processing), and the attenuator (composed of a quarter wave plate and a polariser to control the laser energy), then passes through the axicon lens with cone angle of 175° to realise the transformation of Gaussian beam to Bessel beam. Figure 1(b) shows the geometrical laser path diagram for transforming Gaussian beam into Bessel beam by using axicon lens. When the femto-second laser is incident on the horizontal incident plane of axicon lens, the beam in the upper half will be refracted downward, while the beam in the lower half will be refracted upward, and Bessel beam will be formed in the overlapping area of the two beams. Usually, the power density of the transformed Bessel beam is weak, and the material cannot be removed by it. In order to increase the intensity of Bessel beam, the 4*f* system is used to increase the power density of laser, so as to produce high-quality Bessel beams with significantly enhanced intensity. Specifically, as shown in Figure 1(c), f_1 and f_2 are the focal lengths of lenses L1 and L2, and the distance between the two lens is equal to $f_1 + f_2$. Through this optical path adjustment, the equal proportion of z_{max} (Bessel region) can be reduced. Finally, the transformed Bessel beam is focused on the surface of the diamond grinding wheel fixed on the four-dimensional electric motion platform (the radial jump of the rotary table is 20 μm, and the repeated positioning accuracy of the electromotion table is 5 μm) through the lens (focal length: 25 mm). The composite motion of the grinding wheel is realised by controlling the four-dimensional electromotion table. As shown in Figure 1(d), the laser incident direction is opposite to the rotation direction of the grinding wheel to achieve material removal. A laser range finder, LK-G10, was used to measure the circular run-out of the rotating grinding wheel, and the circular run-out of the envelope formed by the highest point of the abrasive particle on the surface of the protruding binder was measured. The profile accuracy was determined by the circular run-out error of the grinding wheel surface. The surface morphology of grinding wheel was examined by a 3D laser confocal microscope (VK-X200K, Keyence, Japan), we can measure it at room temperature.

2.2 Experimental study on ablation threshold of diamond grinding wheel

2.2.1 Ablation threshold and calculation method of materials

In the process of interaction between laser and material, when the energy density of laser is greater than the ablation threshold of material, the workpiece can achieve effective material removal. By adjusting the incident laser energy, the energy density reaches the ablation threshold of the material. In the ablation centre area, the material is removed by gasification. In the near centre region of ablation, the energy density of laser reaches the threshold of material modification, which can realise the processing of periodic structure. In the peripheral area of laser ablation, the energy density of laser is relatively low, which fails to reach the ablation and modification threshold of the material, and there is no material ablation phenomenon. In this paper, the ablation threshold is calculated by numerical calculation method. By analysing the change of ablation hole diameter on the surface of the material under different laser power, the ablation threshold of the material can be obtained conveniently and quickly. The specific calculation process is as follows:

The femto-second laser after transforming and focusing by the optical path shaping system is Bessel distribution, and its distribution in space can be approximately Gaussian distribution, which is determined by the following formula (Meng et al., 2015):

$$\varphi(r) = \varphi_0 e^{-2r^2/\omega_0^2} \tag{2.1}$$

r is the distance to the spot centre (μm), φ_0 is the energy density of the spot centre (J/cm^2), and ω_0 is the waist radius of the spot. The relationship between the energy density φ_0 of the laser spot and the laser power E_p is: $\varphi_0 = \frac{2E_p}{\pi\omega_0^2}$, the laser energy can be obtained by the average power of the laser: $E_p = \frac{P}{f}$, P is the laser power (W), which can be measured by power metre, and f is the laser repetition frequency (Hz), so it can be obtained: $\varphi_0 = \frac{2P}{f \cdot \pi\omega_0^2}$.

Because the ablation threshold of laser is the minimum energy density to achieve material removal, it can be obtained (Meng et al., 2015),

$$\varphi_{th} = \varphi_0 e^{-D^2/2\omega_0^2} \tag{2.2}$$

φ_{th} is the ablation threshold of the material (J/cm^2), and D is the diameter of the spot (μm), which can be obtained,

$$D^2 = 2\omega_0^2 \ln\left(\frac{\varphi_0}{\varphi_{th}}\right) = 2\omega_0^2 \left(\ln\varphi_0 - \ln\varphi_{th}\right) \tag{2.3}$$

Substitute $\varphi_0 = \frac{2E_p}{\pi\omega_0^2}$ into formula (2.3),

$$D^2 = 2\omega_0^2 \left(\ln E_p + \ln\frac{2}{\pi\omega_0^2} - \ln\varphi_{th}\right) = 2\omega_0^2 \ln E_p + 2\omega_0^2 \ln\frac{2}{\pi\omega_0^2} - 2\omega_0^2 \ln\varphi_{th} \tag{2.4}$$

The φ_{th} and ω_0 in formula (2.4) are the intrinsic properties of the material and remain unchanged, so formula (2.4) is a linear function with E_p as the independent variable. During the experiment, the ablation of the material is carried out by changing the laser energy, and the ablation diameters corresponding to different energies are recorded. The scatter plot of lnE_p and D^2 is drawn, and the corresponding relationship between them is obtained by linear fitting. Then the ablation threshold and waist radius of the material are obtained by linear calculation. Due to the different materials of bronze binder and diamond, the removal of materials after laser ablation is different. Therefore, the ablation thresholds of bronze binder and diamond are calculated in this paper for the subsequent experiments.

2.2.2 Design of ablation threshold experiment

Using the Bessel femto-second laser processing system shown in Figure 1, the laser power is adjusted by the power attenuator, and the power is measured in real time by the power metre. The repetition frequency of the femto-second laser remains unchanged at 1 kHz. The ablation morphology obtained on the material surface under a single pulse is relatively shallow, and it is difficult to accurately measure the diameter of micropores.

Therefore, 100 pulses are selected for this experiment, and the specific experimental parameters are shown in Table 2.

Table 2 Experimental parameters for Bessel beam single point ablation

Experiment parameters	*Number of pulses*	*Laser power P/mW*
Numerical value	100	100, 150, 200, 250, 300
		20, 40, 60, 80, 100

Before the experiment, the diamond wafer and bronze bond block are ultrasonically cleaned for 10 min (using anhydrous ethanol) to reduce the adhesion of other impurities and dried. The treated diamond and bronze bonded blocks are fixed on a three-dimensional precision motion platform. The laser focus is realised by controlling the horizontal movement of the platform, and the material is ablated by selecting the processing position.

2.3 Experimental design of grinding wheel dressing

Due to the randomness of the protrusion height distribution of the abrasive particles on the grinding wheel surface, in the laser dressing process, the small focal depth may not effectively remove the binder and diamond materials. Therefore, we transform Gaussian beam into Bessel beam to obtain long focal depth.

The spatial intensity distribution of the incident Gaussian beam can be described as (Luo et al., 2015)

$$I_G(r, z) = I_0 \left(\frac{\omega_0}{\omega_z} \right)^2 \exp\left(-\frac{2r^2}{\omega_z^2} \right) \tag{2.5}$$

I_0 is the intensity of incident light at the origin, r is the radial axis in cylindrical coordinate system, ω_0 and ω_z are the waist radius and beam radius of incident Gaussian beam, respectively. Based on the above assumptions, the intensity distribution of the first-order Bessel beam along the optical axis can be obtained by integrating the energy field of the incident Gaussian beam and performing differential processing along the optical axis. The equation is derived as follows (Brzobohatý et al., 2008):

$$\begin{aligned} I_B(0, z) &= \left[\iint I_0 \exp\left(-2r/\omega_0\right)^2 r \cdot d\delta dr \right] \Big/ dz \\ &= \left[2\pi r I_0 \exp\left(-2r/\omega_0\right)^2 \cdot dr \right] \Big/ dz \\ \xrightarrow{r=z\cdot\tan\theta} &= \left(2\pi I_0 \tan^2\theta \cdot z\right) \exp\left[-2\left(z \cdot \tan\theta/\omega_0\right)^2 \right] \end{aligned} \tag{2.6}$$

z is the central axis of the cylindrical coordinate system, θ is the inclination angle of the first-order Bessel beam as shown in the figure. The spatial intensity distribution of the Bessel beam generated by the axicon lens can be obtained by adding the boundary constraint, namely equation (2.6), to the ideal Bessel beam (Bessel function of the first kind) and introducing the wave vector parameter (Duacastella et al., 2012; Alexeev et al., 2010). Its function expression is shown in equation (2.7), k is the wavenumber ($k = 2\pi/\lambda$), $J_0(x)$ is the zero-order Bessel function of the first kind, and $\Gamma(x)$ is the gamma function.

$$I_B(r,z) = 2k\pi I_0 \tan^2\theta z \cdot e^{-2(z\tan\theta/\omega_0)^2} \cdot J_0^2[kr\tan\theta]$$
$$J_0(x) = \sum_{m=0}^{\infty} \frac{(-1)^m}{m!\Gamma(m+1)}\left(\frac{x}{2}\right)^{2m} \tag{2.7}$$

In the defocusing amount experiments, the laser power density was set to 3.75 × 10^5 W/cm^2, the rotation speed of the grinding wheel was 10 r/min, the axial scanning speed of the laser was 0.03 mm/min, and the scanning period of the laser beam was set to two times (the width of the axial scanning through a rectangular groove was set to one scanning period). The grinding wheel was tangentially profiled with different defocusing amounts.

The fixed number of laser scanning and the rotation speed of the grinding wheel are ensured, and the laser power is changed. The grinding wheel is subjected to tangential ablation processing (rectangular groove with width of 400 μm) with different axial scanning speeds as variables. The experimental parameters are listed in Table 3. The surface morphology of the grinding wheel is observed to evaluate the dressing quality of the grinding wheel, namely, the protrusion height of the abrasive grain and the round run-out of the grinding wheel. After changing the laser power and axial scanning speed, the single factor variable experiment is carried out, and the optimised experimental parameters are selected. The grinding wheel speed is changed, and the tangential ablation processing of the grinding wheel is carried out with different laser axial scanning speed as variables to further evaluate the surface dressing quality of the grinding wheel.

Table 3 The experimental parameters of laser dressing

Laser dressing parameters	
Laser power density/(×10^5 W/cm^2)	3.75–5.75
Defocusing amount/mm	(–0.6)–(+0.7)
Axial scan speed/(mm/min)	0.05–0.01
Grinding wheel speed/(r/min)	3–10
Groove width/μm	400

3 Results and discussion

3.1 Ablation threshold analysis of diamond grinding wheel

Different laser energy was used to ablate the material, and the diameter of the ablation hole was measured and averaged. It can be obtained from formula (2.4) that the logarithm of the ablation power is linearly related to the square of the diameter of the ablation hole. Therefore, after measuring the diameter of the ablation hole on the surface of diamond and bronze binder, the scatter plot is drawn by calculating the square of the diameter of the hole and the logarithm of the corresponding laser energy, and the logarithm of the laser power and the square of the diameter of the ablation hole are linearly fitted, as shown in Figure 2. According to the fitted linear slope k, the beam waist radius with different materials were obtained by the formula $\omega_0 = \sqrt{k/2}$ as 26.82 μm and 32.83 μm. Next, we established the scatter diagram between D^2 and $\ln\varphi_0$ according to the

relationship between formula (2.3) E_p and φ_0. At the same time, let the independent variable of the fitting line be zero, $b = -2\omega_0^2 \ln \varphi_{th}$, $\varphi_{th} = e^{-b/2\omega_0^2} = e^{-b/k}$ under the action of laser with wavelength of 800 nm and pulse duration of 35 fs, the ablation thresholds of diamond and bronze binder under 100 pulses were obtained as follows: 0.091 J/cm^2 and 0.035 J/cm^2.

3.2 *Defocusing amount*

The results of tangential dressing of grinding wheel by Bessel beam are shown in Figure 3. When the defocusing amount was –0.6 mm, the binder can only be removed slightly, and the diamond abrasive particles can hardly be removed, so the dressing quality is poor, as shown in Figure 3(a). When the defocusing amount was kept between –0.6 mm and +0.6 mm, the binder was effectively removed and the cutting traces on the abrasive surface can be observed, as shown in Figures 3(b)–3(f); when the defocusing amount was +0.7 mm, the removal effect of abrasive particles and binder was poor, and the surface of diamond abrasive particles loosed the original yellow lustre and was covered by black material coating (Chen et al., 2015b), as shown in Figure 3(g).

Figure 2 The relationship between the logarithm of the pulse energy and the square of the diameter, (a) diamond (b) bronze bond (see online version for colours)

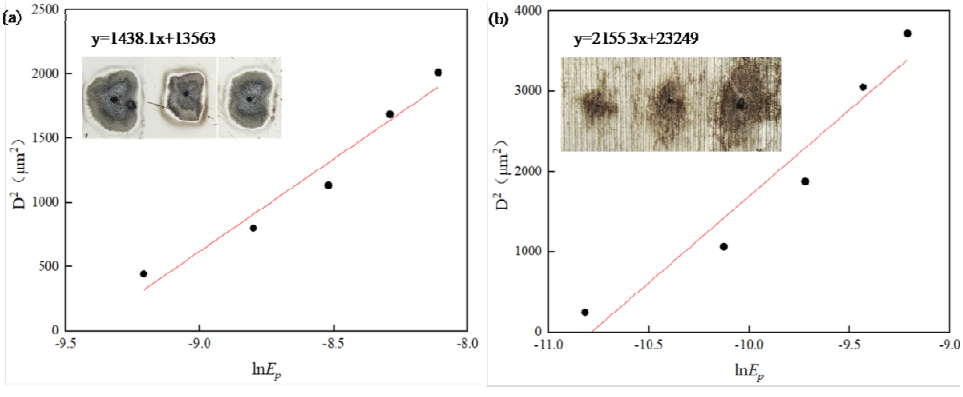

The results of tangential dressing of grinding wheel by Gaussian beam are shown in Figure 4. When the defocusing amount was more than –0.1 mm, only the trace removal of binder can be achieved, as shown in Figure 4(a). The common Gaussian beam can achieve better processing effect when the focal depth was 0.4 mm, as shown in Figure 4(b)–4(d), and the Gaussian beam spot diameter was large, which caused serious burns in the actual processing, resulting in low correction accuracy. When +0.3 mm was above, the diamond abrasive particles were completely prominent, almost impossible to remove, and the abrasive particles loosed their original lustre, as shown in Figures 4(e)–4(f). Figure 5 shows that the Bessel beam can be processed in a large focal depth range, and the overall surface quality is better than the Gaussian beam processing results.

Figure 3 (a1)~(g1) Laser microscopy (a2)~(g2) 3D topography (a3)~(g3) Sectional profile of laser irradiated grinding wheel surface under different defocusing amounts of Bessel beams, (a) –0.6 mm (b) –0.4 mm (c) –0.2 mm (d) +0.2 mm (e) +0.4 mm (f) +0.6 mm (g) +0.7 mm (see online version for colours)

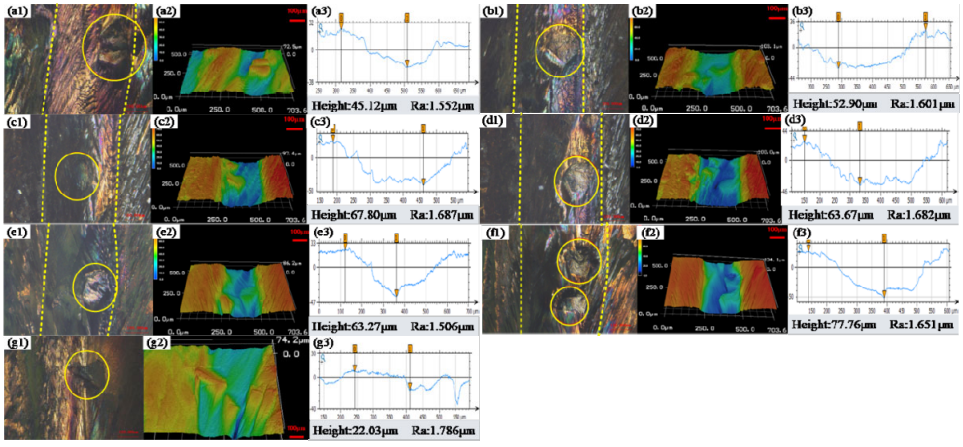

Figure 4 (a1)~(f1) Laser microscopy (a2)~(f2) 3D topography (a3)~(f3) Sectional profile of laser irradiated grinding wheel surface under different defocusing amounts of Gaussian beams, (a) –0.3 mm (b) –0.1 mm (c) +0.1 mm (d) +0.3 mm (e) +0.5 mm (f) +0.7 mm (see online version for colours)

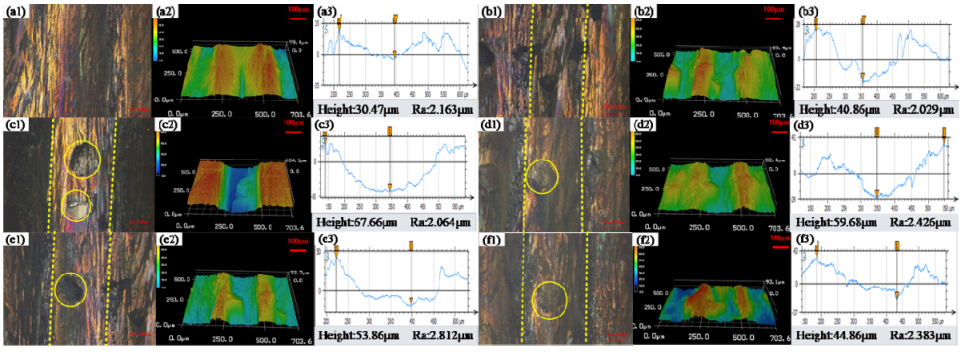

Transforming Gaussian beam into Bessel beam can effectively solve this problem. Laser dressing of grinding wheel can be realised in the range of 1.2 mm focal depth, and the degree of graphitisation of diamond abrasive particles can be reduced. Therefore, laser dressing with Bessel beam can not only ensure small spot diameter and improve dressing accuracy, but also avoid frequent adjustment of the relative position of the grinding wheel in the dressing process by using the characteristics of long focal depth.

3.3 Laser dressing experiments of grinding wheel

Through the calculations in Subsection 3.1, Bessel beam has small spot diameter and longer focal depth, and it can achieve better processing effect in a large range of defocusing. Therefore, the single-factor variable experiments were conducted by changing the laser power, the wheel speed and the wheel axial scanning times.

Figure 5 Surface roughness obtained under different defocusing amounts, (a) Bessel beam (b) Gaussian beam (see online version for colours)

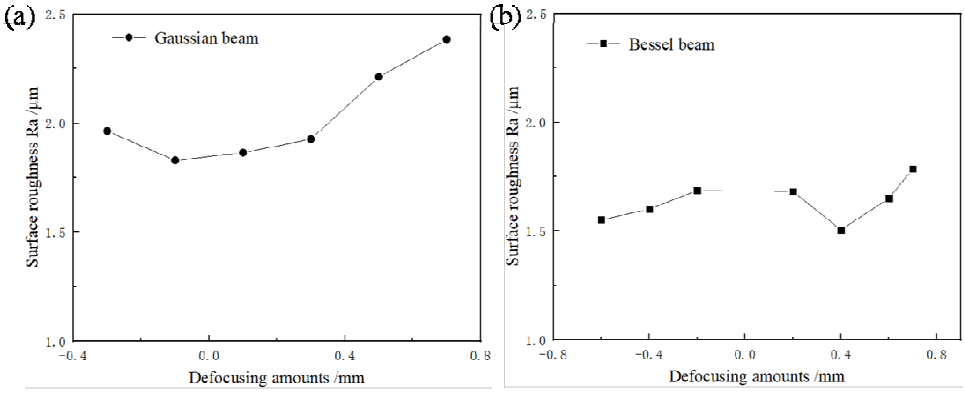

3.3.1 Influence of laser power and axial scanning speed

In the tangential dressing of bronze bonded diamond grinding wheel, the laser power is one of the most critical processing parameters, which is closely related to the surface profiling accuracy and grinding performance of the grinding wheel. The observation results of the laser microscope on the surface of the grinding wheel are shown in Figure 6. When the laser power density was 5.75×10^5 W/cm^2, the axial scanning speed of 0.04 mm/min was set, as shown in Figure 6(a). Most diamond grains was protruded from the binder surface by 15–20 μm, and the groove depth was about 80 μm; when the axial scanning speed was 0.03–0.01 mm/min, as shown in Figures 6(b)–6(d), the groove depth reached about 185 μm, and the diamond grains were basically flattened. The cutting effect of laser can be observed, that is, the purpose of profiling was achieved. The relationship between axial scanning speed and groove depth under different laser powers is shown in Figure 7. However, a layer of black material is attached to the surface of the abrasive particles, and the diamond loses its original lustre. The reason is that the thermal stability of diamond in the air is poor, and high power density will lead to high temperature in the laser ablation zone, which aggravates the oxidation and graphitisation of diamond particles (Chen et al., 2010). When the laser power density was 4.75×10^5 W/cm^2, the groove depth was relatively shallow. When the laser axial scanning speed was controlled at 0.04–0.03 mm/min, as shown in Figures 6(e)–6(f), the protrusion height of abrasive grains was 20–25 μm; when the axial scanning speed was 0.02–0.01 mm/min, as shown in Figures 6(g)–6(h), most of the diamond grains were flattened, and there was some graphitisation of the grains, which can achieve the purpose of shaping. When the laser power was 3.75×10^5 W/cm^2, as shown in Figures 6(i)–6(l), changing the axial scanning speed of the laser, the abrasive particles highlighted the surface of the binder by about 20–30 μm, and the removal depth of the binder was basically the same. This is because the laser power density reaches the threshold of the ablation of bronze binder, but it is not enough to ablate and destroy the abrasive, so that the diamond particles are protruding from the surface of the binder, and only a small amount of abrasive particles are removed. When the axial scanning speed was 0.02–0.01 mm/min, due to the high overlap rate of laser scanning, the actual groove width is greater than the original 400 μm, which will affect the profile accuracy of the grinding wheel, and the long dressing time

will also affect the dressing efficiency of the grinding wheel. The material removal rate of grinding wheel under different laser power density and axial scanning speed can be determined by the following formula as shown in Table 4:

$$Q = \frac{V}{T} \tag{3.1}$$

In this formula, Q is material removal rate (mm^3/min), V is material removal volume (mm^3), and T is material removal time (min).

Figure 6 (a1)~(l1) Laser microscope observation (a2)~(l2) 3D profile image (a3)~(l3) Sectional profile of laser images under different laser power density and axial scanning speed experiment conditions, (a)~(d) 5.75×10^5 W/cm^2, 0.04–0.01 mm/min (e)~(h) 4.75×10^5 W/cm^2, 0.04–0.01 mm/min (i)~(l) 3.75×10^5 W/cm^2, 0.04–0.01 mm/min (see online version for colours)

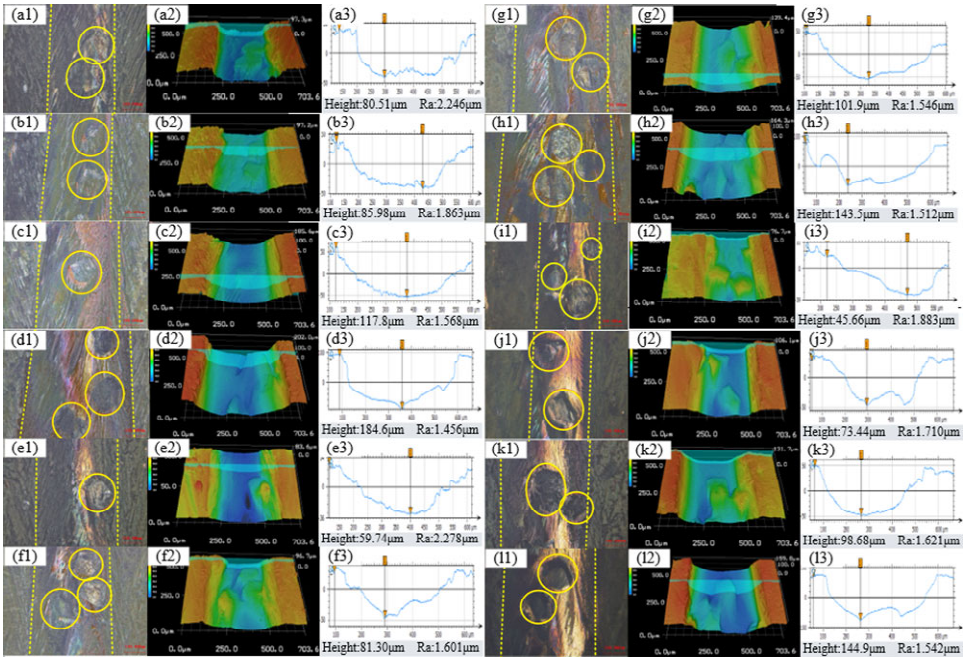

Table 4 Material removal rates at different laser power density and axial scan speeds

Laser power density I_p/(W/cm^2)	*Axial scan speed/(mm/min)*				
	0.01	*0.02*	*0.03*	*0.04*	*0.05*
3.75×10^5	0.0220	0.0289	0.0359	0.0356	0.0203
4.75×10^5	0.0234	0.0320	0.0397	0.0375	0.0235
5.75×10^5	0.0299	0.0357	0.0397	0.0437	0.0313

Figure 8 shows the circular runout error of the wheel surface. When the axial scanning speed of the wheel was 0.03 mm/min and the laser power density was 5.75×10^5 W/cm^2, 4.75×10^5 W/cm^2 and 3.75×10^5 W/cm^2, respectively, the error is measured by the laser rangefinder at three different experiment sections before and after dressing. Figure 8(a)

shows the large wheel circular runout (110.5 μm, 63.4 μm and 65.2 μm), which was caused by the uneven distribution of abrasive particles and the random distribution of many pits on the whole wheel surface of the binder. Figure 8(b) shows that after tangential laser dressing, the circular runouts of three grinding wheels with different cross sections decreased to 4.9 μm, 6.2 μm and 5.5 μm, respectively. The profile accuracy of the grinding wheel after surface dressing was high, and the accuracy was sufficient to meet the application requirements of coarse-grained grinding wheels. Under the current experimental conditions, when the average laser power density was 3.75×10^5 W/cm^2 – 4.75×10^5 W/cm^2 and the laser axial scanning speed was 0.03 mm/min, it is the best choice for laser tangential dressing of bronze bonded diamond grinding wheel. At this time, it can not only ensure high contour accuracy, but also ensure the appropriate protrusion height of abrasive grains and realise grinding performance.

Figure 7 (a) Axial scanning speed versus groove depth under different laser power density (b) Axial scanning speed versus abrasive protrusion height under different laser power density (see online version for colours)

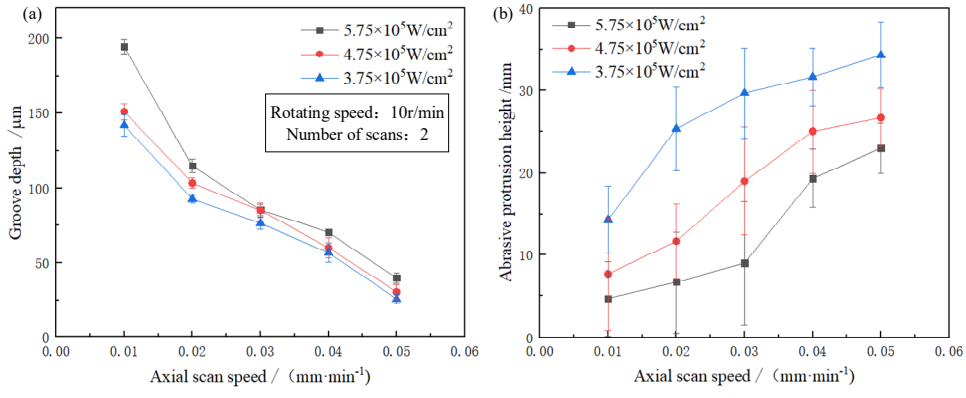

Figure 8 Circular runout error at different positions on the grinding wheel, (a) before profiling (b) after profiling (see online version for colours)

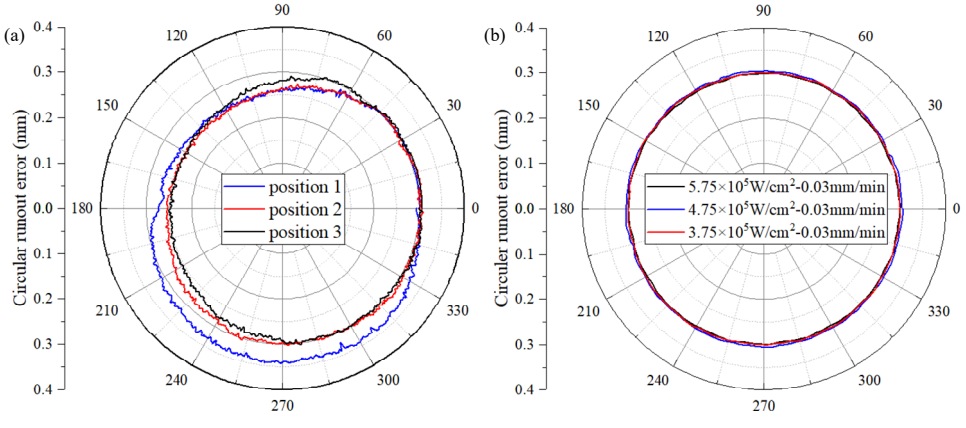

Figure 9 (a1)~(o1) Laser microscope observation (a2)~(o2) 3D profile image (a3)~(o3) Sectional profile of laser images under different grinding wheel rotational speed and axial scanning speed experiment conditions, (a)~(e) 3 r/min, 0.05~0.01 mm/min (f)~(j) 6 r/min, 0.05~0.01 mm/min (f)~(j) 10 r/min, 0.05~0.01 mm/min (see online version for colours)

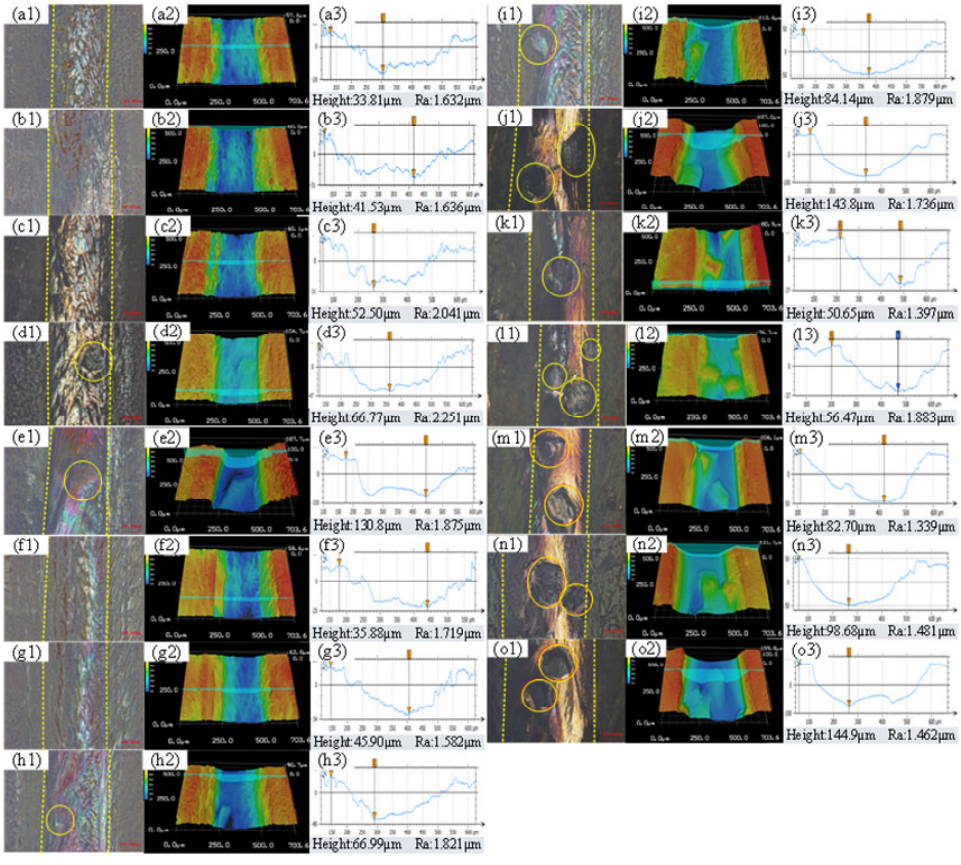

Table 5 Material removal rates at different wheel speeds and axial scan speeds

Wheel speed/(r/min)	*Axial scan speed/(mm/min)*				
	0.01	*0.02*	*0.03*	*0.04*	*0.05*
3	0.0185	0.0225	0.0211	0.0288	0.0211
6	0.0206	0.0225	0.0300	0.0288	0.0266
10	0.0220	0.0289	0.0359	0.0356	0.0203

3.3.2 Influence of grinding wheel speed and axial scanning speed

After changing the laser power density and axial scanning speed for single factor variable experiments, the optimised experiments parameters are selected. The laser power density was set to 3.75×10^5 W/cm^2. The rotation speed of the grinding wheel was changed, and the tangential ablation of the grinding wheel was carried out with different laser axial scanning speeds as variables. The laser microscope observation results of the grinding

wheel surface are shown in Figure 9. When the grinding wheel speed was 3 r/min and 6 r/min, the removal depth of the binder had little change. When the axial scanning speed was 0.05–0.03 mm/min, the bronze binder can only be removed slightly. Due to the low abrasive concentration, diamond abrasive particles can not be observed basically. When the axial scanning speed was controlled at 0.02–0.01 mm/min, the abrasive particles can highlight the binder surface by 20–30 μm. Due to the low rotational speed, the overlapping rate of trajectory scanning was too low, and the profile accuracy of the grinding wheel surface was reduced. When the rotational speed of the grinding wheel was 10 r/min and the axial scanning speed was 0.04–0.02 mm/min, the abrasive particles highlight the binder surface about 30 μm, and at this time, the abrasive particles had a suitable protrusion height. When the axial scanning speed was 0.01 mm/min, the abrasive particles were basically flattened, but the abrasive particles loosed their original lustre and were covered by a layer of black paint, and the dressing efficiency was too low. The relationship between axial scanning speed and groove depth under different grinding wheel speeds are shown in Figure 10. Under the condition of constant axial scanning speed of grinding wheel, the slower the grinding wheel speed is, the smaller the depth of binder removal is, it will reduce the material removal efficiency. The material removal efficiency is shown in Table 5. Therefore, too low rotation speed will not only reduce the overlap rate of axial scanning trajectory, but also reduce the material removal efficiency.

Figure 10 (a) Axial scanning speed versus groove depth under different grinding wheel speed (b) Axial scanning speed versus abrasive protrusion height under different grinding wheel speed (see online version for colours)

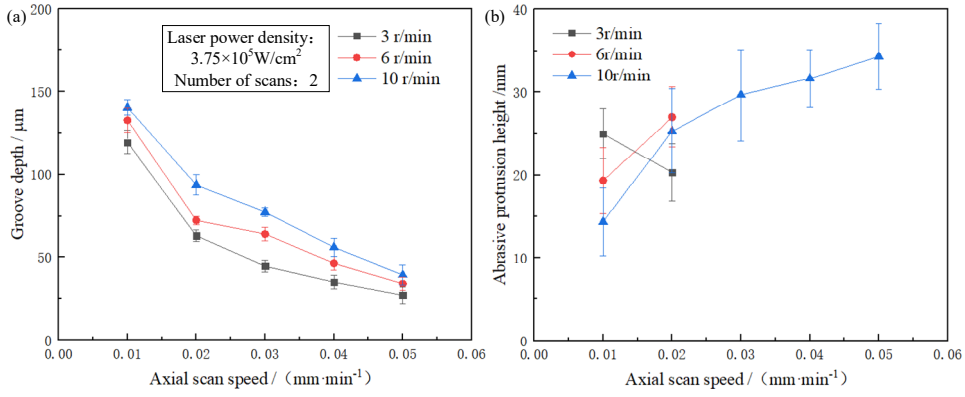

4 Conclusions

In this study, the laser tangential dressing experiments of bronze bonded diamond grinding wheel are carried out by using Bessel beam. The principle of optical path transforming from Gaussian beam, which is generated by femto-second laser, into Bessel beam is studied. The tangential dressing quality of grinding wheel under different defocusing amounts of Gaussian beam and Bessel beam is observed. The removal effect of grinding wheel binder and diamond abrasive particles under different laser power density, axial scanning speed and wheel speed is analysed. The main conclusions are as follows:

1 Single-point ablation experiments of diamond and bronze binders are carried out using Bessel beams. The waist radius of diamond and bronze binders are 26.82 μm and 32.83 μm, and the ablation thresholds of materials are 0.091 J/cm^2 and 0.035 J/cm^2, respectively.

2 When ordinary Gaussian beam is used for tangential dressing of grinding wheel under different defocusing amounts, the better processing effect can be achieved when the focal depth is 0.4 mm. The diameter of Gaussian beam spot is large, and the burn is serious in the actual processing process, resulting in low profiling accuracy. The laser dressing of the grinding wheel can be realised by transforming the Gaussian beam into the Bessel beam in the range of 1.2 mm focal depth, which is several times of the traditional Gaussian beam. It can not only ensure the smaller spot diameter, but also take advantage of the long focal depth of the Bessel beam to avoid frequent adjustment of the relative position of the grinding wheel in the dressing process and improve the dressing efficiency.

3 Laser confocal microscope is used to measure the micro-morphology of the bronze bonded diamond grinding wheel after laser tangential dressing under different laser power density, wheel speed and axial scanning speed. The material removal rates under different experimental conditions are calculated. When the laser power density is 3.75×10^5 W/cm^2 – 4.75×10^5 W/cm^2 and the laser axial scanning speed is 0.03 mm/min, the runout of the grinding wheel is reduced from 64.3 μm to about 6 μm, which can not only make the diamond grains protrude at an appropriate height, but also ensure high profile accuracy. Too low wheel speed will reduce the overlap rates of trajectory scanning and reduce the material removal efficiency.

This study provides a new method and idea for the laser tangential dressing of grinding wheel. In the future, more experiments of laser dressing of grinding wheel will be carried out. After optimising the experimental parameters in the early stage, the optical path transforming and laser dressing system is built on the five-axis linkage ultra-precision machine tool to carry out the profile dressing of the grinding wheel so as to realise the integration of grinding and grinding wheel dressing, and avoid the problems of positioning error and accuracy reduction caused by frequent loading and unloading of the grinding wheel. Ultra-fast laser grinding wheel dressing will gradually replace the traditional mechanical dressing, and has broad application prospects in the field of super-hard grinding wheel and even diamond tool.

Acknowledgements

This work was supported by the Shenzhen Science and Technology Program (Grant No. GJHZ20210705142537003), National Natural Science Foundation of China (No. 51875321), National Key R&D Program of China (No. 2021YFB3203100).

References

Ackerl, N. et al. (2020) 'Ultra-short pulsed laser conditioning of metallic-bonded diamond grinding tools', *Materials and Design*, Vol. 189, p.108530.

Alexeev, I. et al. (2010) 'Application of Bessel beams for ultra-fast laser volume structuring of non transparent media', *Physics Procedia*, Vol. 5, No. Part A, pp.533–540.

Bathe, R. et al. (2014) 'Effect of pulsed laser dressing of metal-bonded diamond wheels on cutting performance', *Materials and Manufacturing Process*, Vol. 29, No. 3, pp.386–389.

Brzobohatý, O. et al. (2008) 'High quality quasi-Bessel beam generated by round-tip axcion', *Optics Express*, Vol. 16, No. 17, pp.12688–12700.

Cai, S et al. (2017) 'Surface metamorphic layer of multi-pulse laser dressing of bronze diamond grinding wheel', China Laser, Vol.44 No.12, pp.1202001.

Chen, B. et al. (2016) 'In-situ precision forming and dressing technology of resin-based arc diamond grinding wheels', *Journal of Mechanical Engineering*, Vol. 52, No. 11, pp.193–200.

Chen, G.Y. et al. (2005) 'Acousto-optic Q-switched YAG pulsed laser sharpening and shaping bronze diamond grinding wheel', *Journal of Mechanical Engineering*, Vol. 41, No. 4, pp.175–179.

Chen, G.Y. et al. (2010) 'Experiment and numerical simulation study on laser truing and dressing of bronze-bonded diamond wheel', *Optics and Lasers in Engineering*, Vol. 48, No. 3, pp.295–304.

Chen, G.Y. et al. (2013) 'Pulse fiber laser sharpening bronze diamond grinding wheel', *China Laser*, Vol. 40, No. 7, p.703002.

Chen, G.Y. et al. (2015a) 'Experimental study on fiber laser radial dressing and grinding of resin bond CBN grinding wheel', *China Laser*, Vol. 42, No. 2, p.203008.

Chen, G.Y. et al. (2015b) 'Online tangential laser profiling of coarse-grained bronze-bonded diamond wheels', *The International Journal of Advanced Manufacturing Technology*, Vol. 79, pp.1477–1482.

Chen, G.Y. et al. (2019) 'Fiber laser CNC tangential turing V-shaped concave diamond grinding wheel system based on machine vision technology', *The International Journal of Advanced Manufacturing Technology*, Vol. 104, No. 7, pp.4077–4090.

Chu, D.K. et al. (2019) 'Superamphiphobic surfaces with controllable adhesion fabricated by femto-second laser Bessel beam on PTFE', *Advanced Materials Interfaces*, Vol. 6, No. 14, p.1900550.

Chu, D.K. et al. (2020) 'Ablation enhancement of fused silica glass by femto-second laser double-pulse Bessel beam', *Journal of the Optical Society of America B*, Vol. 37, No. 11, pp.3535–3541.

Deng, H. and Zhou, X. (2019) 'Dressing methods of superabrasive grinding wheels: a review', *Journal of Manufacturing Processes*, Vol. 45, pp.46–69.

Deng, H. et al. (2014a) 'Current situation and prospect of laser dressing technology for superabrasive grinding wheels', *Intense Lasers and Particle Beams*, Vol. 26, No. 7, p.79002.

Deng, H. et al. (2014b) 'Processing parameter optimization for the laser dressing of bronze-bonded diamond wheels', *Applied Surface Science*, Vol. 290, pp.475–481.

Deng, H. et al. (2016) 'Online efficient and precision laser profiling of bronze-bonded diamond grinding wheels based on a single-layer deep-cutting intermittent feeding method', *Optics & Laser Technology*, Vol. 80, pp.41–50.

Deng, H. et al. (2019) 'A theoretical and experimental study on the pulsed laser dressing of bronze-bonded diamond grinding wheels', *Applied Surface Science*, Vol. 314, No. 10, pp.78–89.

Dold, C. et al. (2011) 'A study on laser touch dressing of electroplated diamond wheels using pulsed picosecond laser sources', *CIRP Annals*, Vol. 60, No. 1, pp.363–366.

Dražumeric, R. et al. (2018) 'Truing of diamond wheels – geometry, kinematics and removal mechanisms', *CIRP Annals – Manufacturing Technology*, Vol. 67, No. 1, pp.345–348.

Du, H. et al. (2016) 'Design of fiber laser on-line shaping diamond grinding wheel inspection system', *Laser Technology*, Vol. 40, No. 6, pp.930–934.

Duacastella, M. et al. (2012) 'Bessel and annular beams for materials processing', *Laser & Photonics Reviews*, Vol. 6, No. 5, pp.607–621.

Guo, B. et al. (2022) 'Pulse laser precision truing of the V-shaped coarse-grained electroplating CBN grinding wheel', *Materials & Design*, Vol. 217, p.110650.

Guo, B. et al. (2016) 'Research progress of surface structured grinding wheel grinding technology', *Journal of Harbin Institute of Technology*, Vol. 48, No. 7, pp.1–13.

Guo, B. et al. (2014a) 'Surface micro-structuring of coarse-grained diamond wheels by nanosecond pulsed laser for improving grinding performance', *International Journal of Precision Engineering and Manufacturing*, Vol. 15, No. 10, pp.2025–2030.

Guo, B. et al. (2014b) 'Ultra-precision grinding of non-binder tungsten carbide aspheric molds', *Journal of Mechanical Engineering*, Vol. 50, No. 13, pp.190–195.

Guo, B. et al. (2018) 'Improvement of precision grinding performance of CVD diamond wheels by micro-structured surfaces', *Ceramics International*, Vol. 44, No. 14, pp.17333–17339.

Hosokawa, A. et al. (2006) 'Laser dressing of metal bonded diamond wheel', *CIRP Annals*, Vol. 55, No. 1, pp.329–332.

Jackson, M.J. et al. (2003) 'Laser dressing of vitrified aluminium oxide grinding wheels', *British Ceramic Transactions*, Vol. 102, No. 6, pp.237–245.

Liu, J.P. et al. (2017) 'Experimental study on pulse laser dressing of V-shaped concave bronze diamond wheel', *Applied Laser*, Vol. 37, No. 4, pp.557–562.

Liu, W.C. et al. (2020) 'Research on water-film assisted pulsed laser machining technology of CVD diamond coated tools', *Precision Manufacturing and Automation*, Vol. 1, pp.16–22.

Luo, Z. et al. (2015) 'One-step fabrication of annular microstructures based on improved femto-second laser Bessel-Gaussian beam shaping', *Applied Optics*, Vol. 54, No. 13, pp.3943–3947.

Mei, L.F. et al. (2009) 'Measurement of YAG laser absorptance by artificial diamond and cubic boron nitride', *Optics & Laser Technology*, Vol. 41, No. 6, pp.770–777.

Meng, X. et al. (2015) *The Study of Femto-Second Laser Ablation Process and Surface Morphology of Solid Materials*, Shandong Normal University.

Meyer, R. et al. (2020) 'Single-shot ultra-fast laser processing of high-aspect-ratio nanochannels using elliptical Bessel beams', *Optics Letters*, Vol. 42, No. 21, pp.4307–4310.

Okamoto, Y. et al. (2019) 'High surface quality micro machining of monocrystalline diamond by picosecond pulsed laser', *CIRP Annals – Manufacturing Technology*, Vol. 68, No. 1, pp.197–200.

Walter, C. et al. (2012) 'Dressing and truing of hybrid bonded CBN grinding tools using a short-pulsed fibre laser', *CIRP Annals*, Vol. 61, No. 1, pp.279–282.

Wegener, K. et al. (2011) 'Conditioning and monitoring of grinding wheels', *CIRP Annals – Manufacturing Technology*, Vol. 60, No. 2, pp.757–777.

Weingaertner, E. et al. (2010) 'On-machine wire electrical discharge dressing (WEDD) of metal-bonded grinding wheels', *The International Journal of Advanced Manufacturing Technology*, Vol. 49, No. 9, pp.1001–1007.

Xie, J. and Dang, X.M. (2008) 'Arc-shaped diamond grinding wheel's numerically controlled alignment forming dressing test', *Journal of Mechanical Engineering*, Vol. 44, No. 2, pp.102–107.

Xie, X.Z. et al. (2004) 'Dressing of resin-bonded super abrasive grinding wheels by means of acousto-optic Q-switched pulse Nd: YAG laser', *Optics and Laser Technology*, Vol. 36, No. 5, pp.409–419.

Yao, Z.X. et al. (2018) 'Research on GC cup truing technology of super-hard grinding wheel', *Key Engineering Materials*, Vol. 764, pp.408–415.

Yung, K.C. et al. (2003) 'The laser dressing of resin-bonded CBN wheels by a Q-switched Nd: YAG laser', *The International Journal of Advanced Manufacturing Technology*, Vol. 22, No. 7, pp.541–546.

Zhang, C.Y. et al. (2016) 'Ultra-precision grinding of AlON ceramics: surface finish and mechanisms', *Journal of the European Ceramic Society*, Vol. 39, No. 13, pp.3668–3676.

Zhang, Z.Z. et al. (2019) 'A novel technique for dressing metal-bonded diamond grinding wheel with abrasive waterjet and touch truing', *The International Journal of Advanced Manufacturing Technology*, Vol. 93, pp.3063–3073.

Zhao, Q.L. and Guo, B. (2011) 'Ultra-precision grinding technology of microstructure optical functional element mold', *Journal of Mechanical Engineering*, Vol. 47, No. 21, pp.177–185.

Zhou, L. et al. (2019) 'Dressing technology of arc diamond wheel by roll abrading in aspheric parallel grinding', *The International Journal of Advanced Manufacturing Technology*, Vol. 105, No. 4, pp.2699–2706.